

Edge-Native Generative De-identification: Inversion-Free Flow for Privacy-Preserving Federated Skin Image Analysis

Konstantinos Moutselos^{*1} [0000-0002-6759-8540] and Ilias Maglogiannis¹ [0000-0003-2860-399X]

¹ University of Piraeus, Dept. of Digital Systems, Piraeus 18534, Greece
{kmouts; imaglo}@unipi.gr

Abstract

The deployment of Federated Learning (FL) in clinical skin image analysis is hindered by the dual challenge of protecting patient anonymity while preserving fine-grained diagnostic features. Traditional de-identification methods often degrade pathological fidelity, whereas standard generative approaches require computationally expensive inversion processes that are unsuitable for resource-constrained edge devices. This study proposes a federated-ready framework for identity-agnostic pathological preservation that operates as a client-side privacy firewall. Using inversion-free Rectified Flow Transformers (FlowEdit), we perform high-fidelity identity transformation in near real-time (<20s), making it viable for local deployment on hospital nodes. A counterfactual segment-by-synthesis mechanism that generates “healthy” and “pathological” twin pairs locally is introduced to ensure the safety of shared gradients. This allows the extraction of differential erythema masks that are mathematically stripped of biometric markers and semantic noise (e.g., jewelry). Our pilot validation on high-resolution clinical samples demonstrates an Intersection over Union (IoU) stability > 0.67 across synthetic identities. By enabling the generation of privacy-compliant “Digital Twins” at the edge, this framework neutralizes gradient leakage risks at the source, paving the way for secure, high-precision skin image analysis FL.

1. Introduction

The integration of Generative AI into dermatological analysis models promises to democratize diagnostic access, building on a growing body of work in automated detection [1] for diseases such as dermatitis and vitiligo [2]. However, widespread adoption is hampered by the ethical imperative of patient privacy. Unlike radiological scans, which can be easily anonymized, facial skin images contain immutable biometric markers—such as ocular structure and craniofacial geometry—that pose severe re-identification risks. Federated Learning (FL) offers a

promising solution by training models on decentralized data; however, a critical vulnerability in the leakage of these biometric features into gradient updates remains. To realize the vision of secure, cross-institutional dermatological AI, we must develop Edge-Efficient mechanisms that decouple the pathological signal (e.g., erythema) from the patient identity before any model training occurs.

1.1. Problem: Identity as Semantic Noise and Privacy Risk

Current zero-shot segmentation models, such as Grounded-SAM [3], operate on semantic priors that are ill-suited for the subtle, diffuse nature of skin inflammation. These models create a dual-failure mode in the FL context:

1. Diagnostic Drift: Pathological erythema is frequently conflated with nonclinical distractors, such as piercings, lips, or natural skin flushing, introducing “noisy labels” into the federated model.

2. Biometric Leakage: The segmentation mask inadvertently encodes identity-specific contours (e.g., the exact shape of an eye or a unique tattoo) by failing to isolate the pathology, exposing the local client to gradient reconstruction attacks [4].

1.2. Proposal: A Client-Side Privacy Firewall

To address this, we introduce a privacy-preserving preprocessing framework designed to sit at the edge of an FL client (e.g., a hospital workstation). The proposed approach uses FlowEdit [5], an inversion-free Rectified Flow Transformer to perform high-fidelity identity transformation. Unlike diffusion models that require computationally intensive inversion loops, our flow-based approach solves a direct ODE, enabling fast, low-compute inference suitable for edge deployment. We create a “privacy firewall” at the data source by shifting the patient’s facial structure to a synthetic surrogate while anchoring the erythema in the latent space (Fig. 1).

We further refine this with the counterfactual Segment-by-Synthesis mechanism [6]. By locally generating a “healthy twin” of the synthetic patient, we extract a

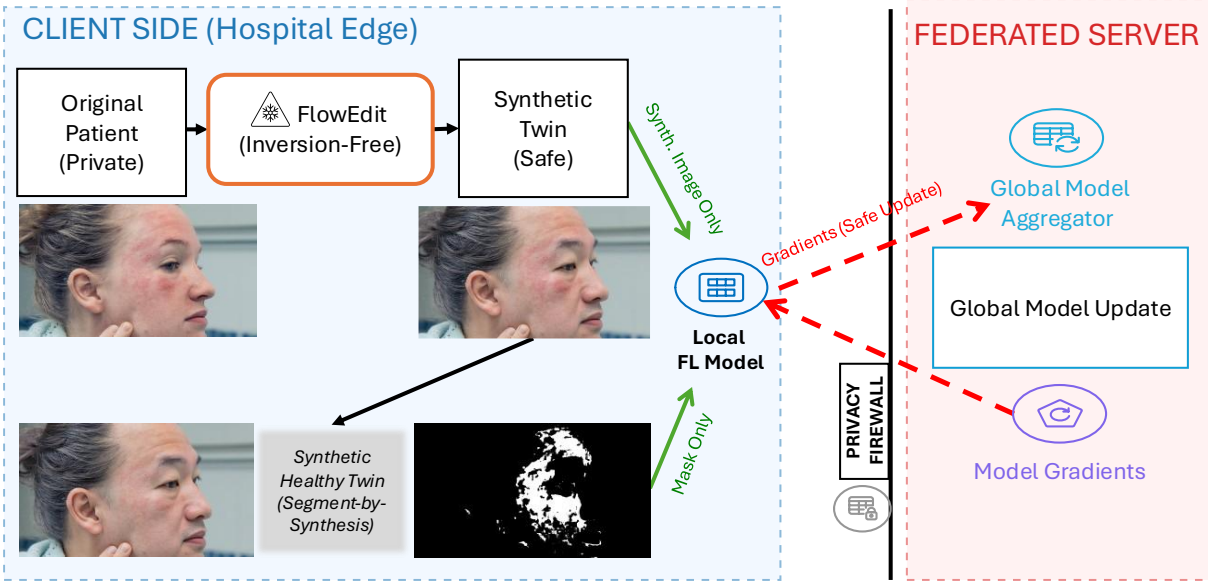


Figure 1: Overview of the Edge-Native De-identification Framework. The original patient image [16] is transformed locally using inversion-free FlowEdit, establishing a privacy firewall at the source. The hospital edge node acts as an active participant, utilizing identity-agnostic synthetic surrogates and differential masks for local model training. Only the resulting model updates (gradients) are transmitted to the global aggregator. This architecture prevents biometric gradient leakage.

differential mask via pixel-wise subtraction. This mask is robust to semantic noise and is stripped of identity-linked features to ensure that only safe, agnostic features are used for FL training.

1.3. Contributions

Our pilot study, which was validated on high-resolution clinical samples, offers three primary contributions:

1. Edge-Efficient De-identification: FlowEdit can shift facial identity with high textural fidelity in less than 20 s, thereby eliminating the computational bottleneck of inversion-based diffusion models and enabling scalable client-side deployment.

2. Noise-Canceling Segmentation: We introduce a synthesis-based differential masking strategy that outperforms Grounded-SAM by successfully filtering out complex distractors (e.g., jewelry, specular reflections) to isolate pure erythema.

3. Privacy-First Data Representation: We propose a “Digital Twin” methodology that creates synthetic, privacy-compliant training pairs. This ensures that the original patient biometric data do not influence the weights of the global model, thereby reducing the risk of root gradient leakage.

2. Related Work

2.1. Privacy Risks in Federated Medical Learning

Federated Learning (FL) enables collaborative model

training without centralizing patient data [7]. However, recent studies on Gradient Inversion Attacks have demonstrated that patient data can often be reconstructed from shared model updates, particularly in sparse datasets like clinical skin imaging data [4]. Differential Privacy (DP) adds noise to gradients to mitigate this, but it degrades the utility of fine-grained diagnostic features [7]. Our work targets a complementary defense: Input-Level De-identification. We neutralize the risk of reconstruction attacks at the root by scrubbing biometric markers at the client source before the data enters the training loop.

2.2. Generative De-identification: From GANs to Inversion-Free Flows

Textural semantics required for dermatological diagnosis are destroyed by traditional anonymization (blurring, pixelation). Generative approaches, such as DeepPrivacy [8], use GANs to swap identities but often suffer from “texture smoothing,” rendering them unsuitable for pathological analysis. To edit real images, recent diffusion models [9] require computationally expensive inversion processes [10], which is impractical for resource-constrained edge devices in hospital networks.

Recent advances in Flow Matching [11] and Rectified Flow [12] have addressed this by linearizing the transport map between distributions. FlowEdit [5] leverages this property to perform inversion-free editing. FlowEdit allows for the modification of global identity semantics while anchoring local textures via guidance by computing the difference between source and target velocity fields directly in latent space, a capability we exploit to

efficiently preserve erythema at the edge.

2.3. Zero-Shot vs. Synthesis-Based Segmentation

In FL settings, data labeling is often unsupervised or semi-supervised. Foundation models, such as the Segment Anything Model (SAM) [13] and its high-fidelity successor HQ-SAM [14] have revolutionized general image segmentation. However, even when combined with open-set detectors, such as the Grounded-SAM [3], these models offer zero-shot segmentation but lack domain specificity, frequently confusing pathology with physiological noise. Although specialized preprocessing algorithms have been successful in removing specific artifacts, such as hair [15], they are often limited to single-noise types. In contrast, Segment-by-Synthesis framework [6] acts as a robust, unsupervised annotator, generating high-quality “Digital Twin” labels locally without requiring manual expert intervention at every clinic.

3. Methodology

We propose a localized preprocessing module that operates on the FL Client (i.e., hospital edge). This pipeline transforms raw patient data into identity-agnostic pathological masks before any gradient computation occurs.

3.1. Inversion-Free Identity Transformation (FlowEdit)

To locally de-identify patient images, we use FlowEdit [5], based on Rectified Flow Transformers. Unlike diffusion models that require iterative inversion to find a noise pivot, FlowEdit solves a direct Ordinary Differential Equation (ODE) to map the source distribution (Patient) to a target distribution (Synthetic Surrogate).

The transformation is governed by the following guided velocity field:

$$\hat{v} = v_{uncond} + \gamma_{src}(v_{src} - v_{uncond}) + \gamma_{tgt}(v_{tgt} - v_{uncond}) \quad (1)$$

This equation represents the mixed guidance mechanism. It calculates the final direction (velocity) that the latent image needs to move at each time step to satisfy both the need to look like the original image (source) and the need to look like the new identity (target). \hat{v} represents the instantaneous velocity vector field that guides the latent pixels from a noised state toward the target edited distribution. It is sent to the ODE solver to generate the de-identified patient. The Unconditional Velocity (v_{uncond}) stands for the model’s prediction when given an empty text prompt (""). It represents the “natural drift” of the model—the direction it would take to generate a generic, coherent image based on general statistics (lighting, composition) without any specific semantic instruction. The Source

Velocity (v_{src}) contains the directions needed to reconstruct the original patient and their pathology. Is the velocity conditioned on the source prompt (e.g., “Photo of a woman with facial erythema”).

The subtraction $v_{src} - v_{uncond}$ isolates the source prompt’s pure semantic signal. Generic image features (v_{uncond}) are removed to leave only the features specific to the patient’s original appearance and disease. The Target Velocity (v_{tgt}) is the velocity conditioned on the target prompt (e.g., “Photo of a man with facial erythema”). It contains the directions needed to hallucinate the new surrogate identity. The subtraction $v_{tgt} - v_{uncond}$ isolates the pure semantic signal of the target prompt (the new gender/identity features). Both γ_{src} and γ_{tgt} are scalar coefficients. The first determines how strongly the model “clings” to the original image details. The Target Guidance Scale (γ_{tgt}) pushes the latent geometry toward the new facial structure (e.g., changing the jawline and eyes) while the source guidance (γ_{src}) fights to maintain the skin texture.

By maintaining high Source Guidance (γ_{src}), we anchor the pathological textures (erythema) while allowing the global facial geometry to shift. This inversion-free architecture reduces the computational overhead, making it viable for deployment on hospital-grade GPUs.

3.2. Counterfactual Segment-by-Synthesis

To generate robust training labels for the FL model, we implement the Segment-by-Synthesis paradigm [6]. For each de-identified image, the client generates a counterfactual healthy twin using the same latent seed but a modified text prompt (“healthy skin”). This yields a pair: (I_{path} , $I_{healthy}$), as illustrated in Figs 2a and 2b. I_{path} is the synthetic pathological twin resulting image, showing the operation: New Identity + Erythema. $I_{healthy}$ is the synthetic healthy twin, showing the operation: New Identity + Healthy Skin. Since identity and lighting are controlled by the fixed seed, the only variance between the two images is the pathology itself:

$$I_{path} = \mathcal{G}(z_{de-id}, \tau_{path}) \quad (2)$$

$$I_{healthy} = \mathcal{G}(z_{de-id}, \tau_{healthy}) \quad (3)$$

The Generator (\mathcal{G}): represents the generative model. In our case, the rectified flow transformer. This function takes a latent noise vector and a text condition as input and outputs a pixel-space image. The de-identified latent code (z_{de-id}) is the shared latent anchor, and this is the specific noise vector (seed) that corresponds to the synthetic surrogate identity we created in the previous step using FlowEdit. This variable appears in both equations. Because the latent code z_{de-id} is held constant, the global facial geometry (nose shape, eye distance, lighting, background)

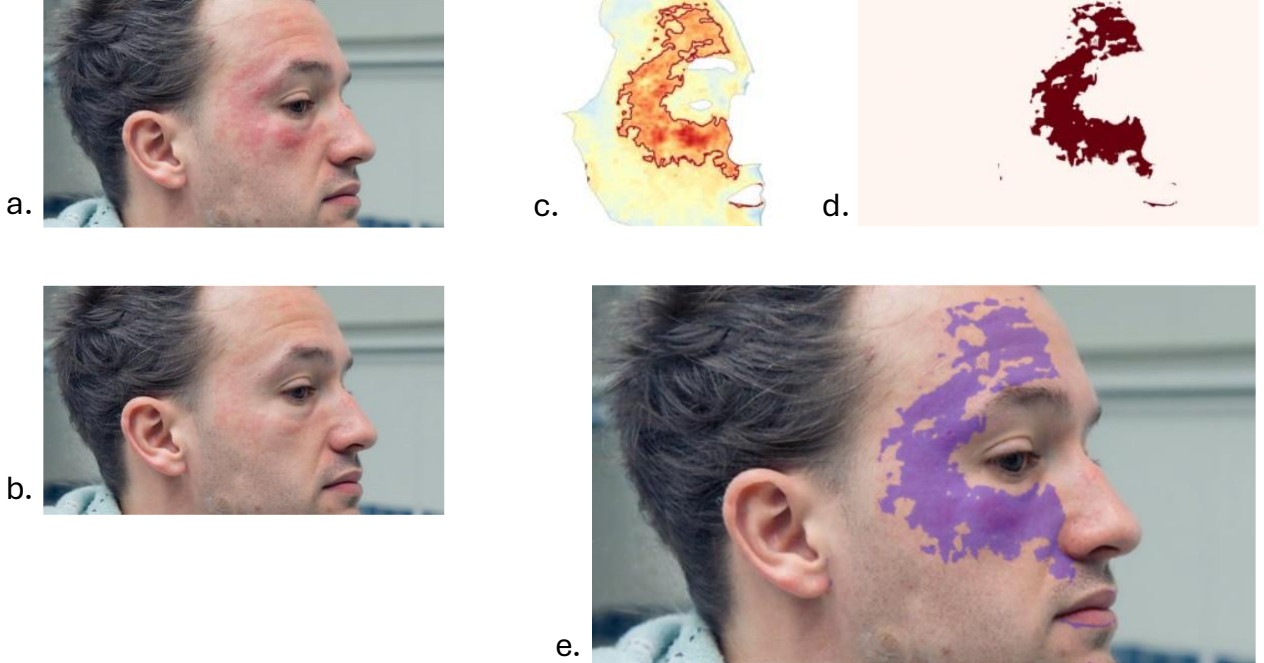


Figure 2: Overview of the Counterfactual Segment-by-Synthesis Workflow. The pipeline isolates the pathological signal by comparing the de-identified subject with a generated “healthy” version of themselves. (a) Synthetic Pathological Twin (I_{path}): The de-identified patient surrogate generated via FlowEdit, retaining the original erythema structure. (b) Synthetic Healthy Twin ($I_{healthy}$): A counterfactual “healthy” variant generated from the identical latent seed, ensuring pixel-perfect anatomical alignment with (a). (c) A-Channel Difference Map: The pixel-wise residual intensity calculated in the CIELAB color space (specifically the α^* channel), which effectively isolates the redness signal from skin pigmentation and lighting. (d) Extracted Mask: The final binary segmentation mask M obtained after applying the optimized dynamic threshold (θ^*). (e) Annotated Surrogate: The resulting high-precision erythema mask overlaid on the synthetic twin, serving as the privacy-preserving ground truth for Federated Learning.

remains identical in both output images. This “locks” the anatomy.

Regarding the conditioning prompts, the pathological prompt (τ_{path}) is the text embedding that describes the clinical condition (e.g., “a photo of a face with skin erythema”). The counterfactual prompt ($\tau_{healthy}$) is the text embedding that describes the healthy state (e.g., “a photo of a face with clear, healthy skin”). This instructs the generator \mathcal{G} to “heal” the skin while keeping everything else the same.

By defining the images $I_{path}, I_{healthy}$ this way, we ensure that the pathology itself is the mathematical difference between the two outputs:

$$I_{path} - I_{healthy} \approx \text{Pure Pathology} \quad (4)$$

Because \mathcal{G} and z_{de-id} are fixed, all anatomical features (which are “noise” for our segmentation task) cancel out during subtraction.

3.3. Differential mask extraction and calibration

The final training target is a binary mask M , derived via pixel-wise subtraction:

$$M = \{p \in \Omega \mid \|I_{path}(p) - I_{healthy}(p)\| > \theta\} \quad (5)$$

Here, Ω represents the entire spatial grid of the image (height \times width), and p represents a single pixel coordinate (x,y) within that grid. Theta (θ) is the dynamic threshold of sensitivity.

This differential approach effectively filters out “identity noise” (e.g., specific eye shapes and piercings) that typically confuses general-purpose segmenters. In a federated setting, only this De-identified Image (I_{de-id}) and the Synthetic Mask (M) are used for local training, ensuring that the original patient biometric data do not influence the model weights.

A dynamic threshold optimization is implemented to refine the segmentation accuracy. The threshold θ is optimized to match the original patient’s erythema mask M_{orig} as closely as possible. The optimal threshold θ^* is selected by maximizing the Intersection over Union (IoU) across the de-identified cohort:

$$\theta^* = \operatorname{argmax}_{\theta} \frac{|M_{orig} \cap M_{de-id}(\theta)|}{|M_{orig} \cup M_{de-id}(\theta)|} \quad (5)$$

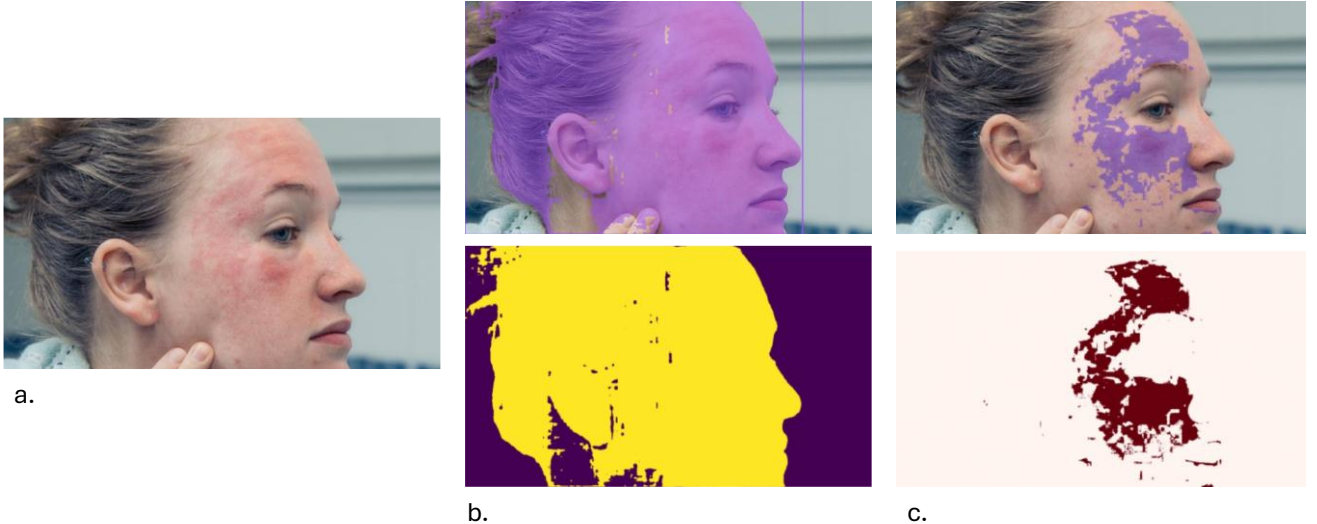


Figure 3: Qualitative comparison on diffuse facial pathology. We benchmark the robustness of our framework against the state-of-the-art Grounded HQ-SAM pipeline on a full-face clinical sample. (a) Original Patient Input (I_{orig}): A high-resolution profile featuring diffuse facial erythema [16]. The pathological signal is subtle and texturally similar to natural skin flushing, posing a challenge for zero-shot segmentation. (b) Baseline (Grounded HQ-SAM): The zero-shot pipeline output. Lacking a comparative “healthy” reference, the model struggles to define the amorphous boundaries of the inflammation, erroneously including non-pathological anatomical features (e.g., lips, hair) or over-segmenting onto healthy skin. (c) Segment-by-Synthesis: Our synthesis-bases privacy-preserving annotation. By subtracting the counterfactual healthy twin, the differential approach cancels out the underlying facial geometry (identity), successfully isolating the pure pathological signal without semantic confusion.

4. Results and Discussion: Pilot Validation

We conducted a pilot validation using high-resolution clinical samples representing challenging edge cases (e.g., facial erythema with occlusion) to assess the feasibility of this pipeline for federated learning.

4.1. De-identification Fidelity

We successfully transformed patient identities (e.g., Female Patient → Male Surrogate) while retaining the structural integrity of the erythema. The inversion-free nature of FlowEdit allowed for inference times of <20 seconds for image resolution 1024x768 (NVIDIA L4), demonstrating the potential for near real-time processing on edge nodes.

4.2. Comparison with the baseline (Grounded-SAM)

We benchmarked our pipeline against a Grounded-SAM pipeline integrated with HQ-SAM [14], with qualitative comparisons shown in Fig. 3. By using HQ-SAM, we ensured that the baseline failure was not due to mask coarseness, but rather the fundamental inability of zero-shot models to distinguish pathology from semantic noise.

Failure Mode: Grounded-SAM frequently misclassifies nonpathological features (lips, piercings, and shadows) as lesions, creating “noisy labels” that degrade FL convergence.

Robustness to artifacts: The Segment-by-Synthesis approach successfully filtered out these distractors. By subtracting the “Healthy Twin,” our method isolated the erythema with pixel-perfect precision, providing clean ground-truth labels for unsupervised learning.

4.3. Mask Stability (IoU Analysis)

We measured the Intersection over Union (IoU) between the original patient’s pathology and the masks generated from the synthetic surrogates:

Facial Image [16] (Case 1): The framework achieved an average IoU of 0.685 ± 0.002 across diverse synthetic identities. The pathological morphology remains visually consistent despite significant changes in the underlying facial geometry (Fig. 2). This stability confirms that the “pathological signal” is invariant to the identity shift, ensuring that FL models trained on these data will generalize to real patients.

Periocular/periorificial Image [17] (Case 2): The method maintained an IoU of 0.674 (Fig. 4), even with high-contrast distractors (piercings), proving robustness against the type of “non-IID” noise common in diverse clinical datasets.

The statistical consistency of the framework was validated by comparing the raw α^* channel distributions across the counterfactual pipelines (Fig. 5). By analyzing the normalized histograms of the skin tones, we quantified the precision of pathology isolation and the stability of the synthetic surrogates. Distribution comparison metrics

indicate that the core clinical signals remain robust, even when transitioning from real-world patient data to fully synthetic domains.

In the initial validation stage (Fig. 5, Left), the distribution of the synthetic healthy version (Fig. 4.1b) is compared directly to the original patient photograph (Fig 4.1a). The high peak density of 0.12 and a standard deviation of 5.69 indicate that the inversion-free transformation successfully performs localized “healing”. By maintaining most of pixels within the patient’s original color gamut (mean $\alpha^* \approx 139$), the model can isolate erythema without distorting the underlying healthy skin texture or lighting of the specific patient.

The comparison between the two synthetic twins (Fig. 5, Right, corresponding to Figs 4.2a and 4.2b), exhibits a

broader variance and a lower peak density (<0.10). This phenomenon is attributed to the “Double Rendering” effect; the pixel-wise stochasticity does not perfectly overlap because both twins are fully synthetic outputs of separate FlowEdit traversals. However, the higher Bhattacharyya coefficient (0.977 vs. 0.959) and lower KS statistic (0.103 vs. 0.130) for this synthetic pair indicate that the two generative outputs are statistically more compatible with each other than the synthetic surrogate is with the original photograph. This confirms that the “Digital Twin” approach provides a highly stable baseline for extracting differential masks that are free from the biometric interference of the original patient data.

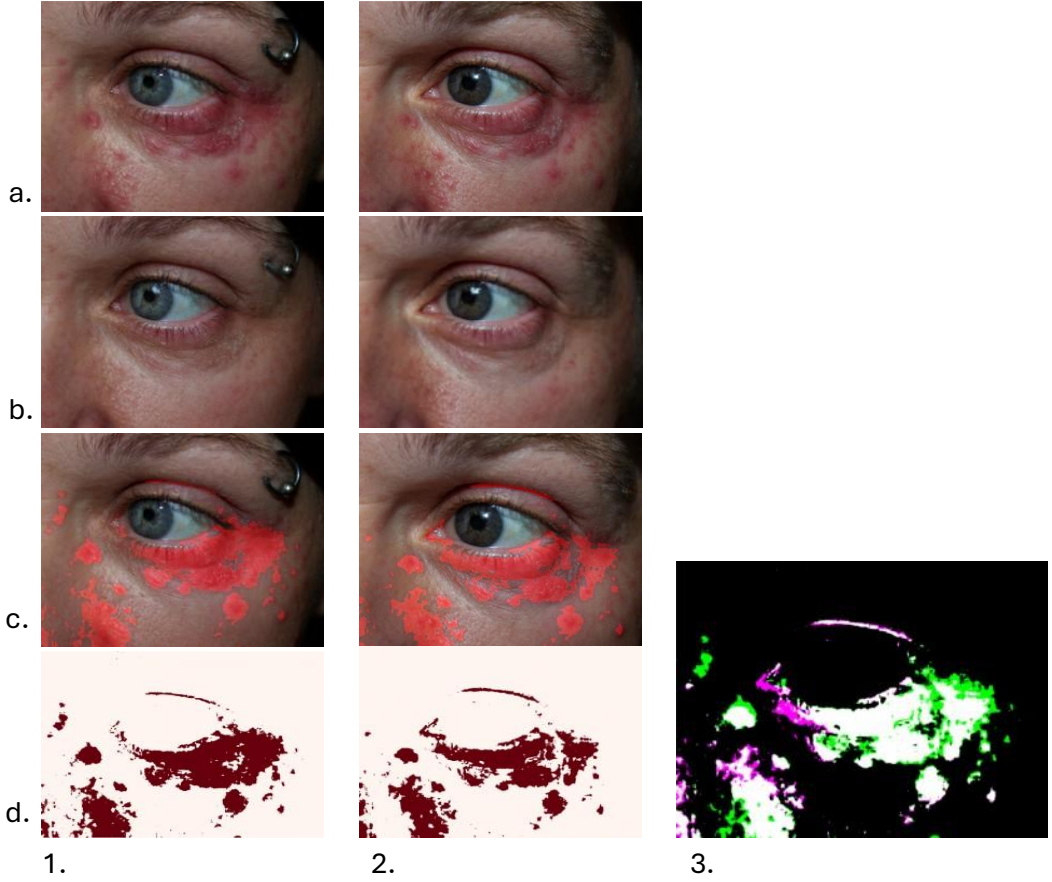


Figure 4: Validation of pathological invariance via mask stability analysis. We demonstrate that the erythema morphology remains consistent even after the identity transformation. Column 1 (Original Identity): The baseline pipeline applied to the patient. (a) Input patient image [17]. (b) Counterfactual healthy twin generated via FlowEdit. (c) Pathological annotation (mask overlay). (d) Binary segmentation mask (M_{orig}). Column 2 (Synthetic Surrogate): The same pipeline applied to the de-identified surrogate. (a) Transformed synthetic identity. (b) Its corresponding healthy twin. (c) Pathological annotation. (d) Binary segmentation mask (M_{syn}). Column 3 (Comparative Overlay): A composite visualization where the Original Mask (M_{orig}) is mapped to Green and the Synthetic Mask (M_{syn}) to Magenta. White Regions: Indicate the Intersection ($M_{orig} \cap M_{syn}$), representing perfect agreement. Green/Magenta fringes: represent morphological deviations (shift). The dominance of white pixels confirms high structural alignment ($IoU > 0.67$), proving that the pathological boundaries are preserved despite the global identity shift.

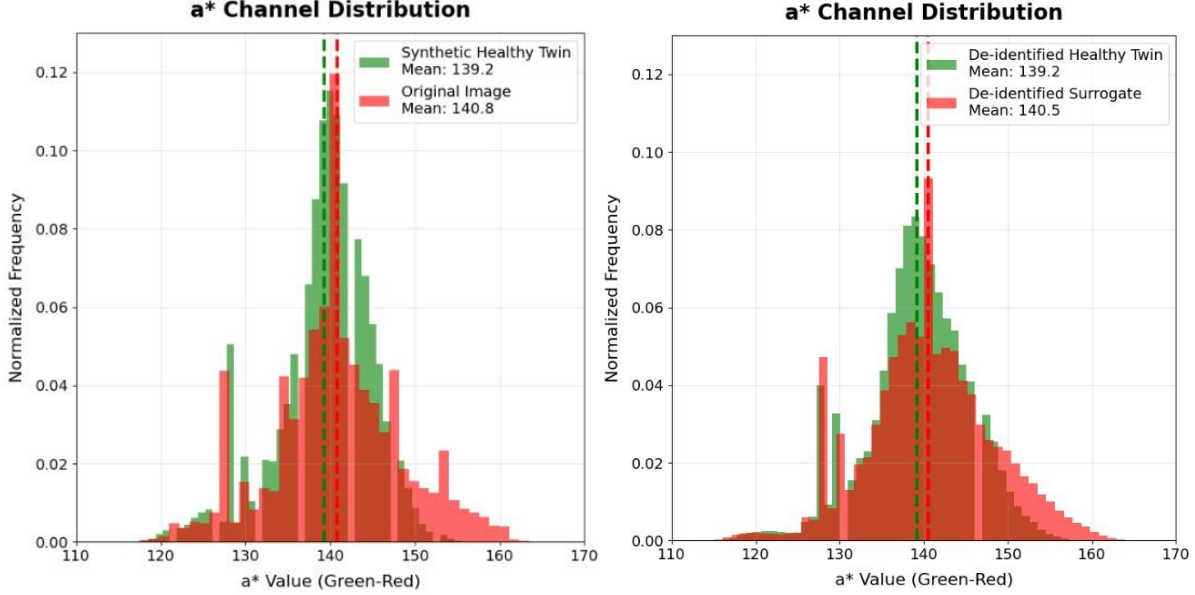


Figure 5: Normalized histograms of a^* channel intensity (Periocular Case): (Left) Original patient vs. synthetic healthy version: the high peak frequency (≈ 0.12) indicates that the inversion-free transformation preserves the specific statistical profile of the patient's original skin tone. (Right) synthetic pathological vs. synthetic healthy twin: The broader distribution (peak < 0.10) reflects the stochastic variance introduced by the dual generative paths, despite sharing a common latent identity.

4.4. Qualitative Analysis: Viewing Angles and Feature Persistence

Our pilot analysis reveals that the efficacy of prompt-guided de-identification is sensitive to the clinical viewing angle. We observed a distinct performance divergence between the Facial Image [16] (Case 1) and the Periocular/periocular Image [17] (Case 2).

The Macro-Lens Challenge: In the close-up regime (Case 2), prompt engineering and hyperparameter tuning proved to be more difficult. The generative model struggled to anchor the semantic context due to the lack of global facial landmarks (e.g., chin contour, hair, background depth). Without these cues, the model occasionally failed to disentangle the “subject” from the “background,” a limitation consistent with previous zero-shot Segment-by-Synthesis observations [6].

Biometric Feature Persistence: We also identified the limitations of fine-grained feature control during single-pass editing. In the full-face sample (Case 1), we explicitly attempted to alter ear morphology—a robust biometric soft-identifier—via prompt engineering. Despite these attempts, the ear structure remained largely unchanged in the synthetic surrogate. The same was observed for the eyebrow morphology in the periocular/periocular image. This indicates that a single velocity field may be insufficient for total biometric suppression.

A potential solution is a multistage de-identification pipeline, where intermediate editing steps specifically target resistant features (e.g., ears or hairline) before the

final pathological consistency check is applied.

4.5. Broader Clinical Generalizability

Although this study primarily focuses on erythema, the Segment-by-Synthesis FL framework is inherently pathology-agnostic. The paradigm can be extended to any clinical condition characterized by visual alterations during disease progression that can be captured via high-resolution clinical imaging.

As highlighted in recent systematic literature reviews [2], the quantitative assessment and automated detection of conditions such as dermatitis, vitiligo, and alopecia areata remain a significant bottleneck in medical informatics. Our framework addresses this gap by enabling the generation of privacy-compliant “Digital Twins” that decouple the pathological signal from the biometric identity of the patient.

The proposed framework is readily extensible to other dermatological conditions, such as:

Pigmentation Disorders: The counterfactual healthy twin logic can be used to restore melanocyte-rich skin regions in vitiligo, allowing for precise quantification of depigmented patches.

Inflammatory Conditions: Hair-loss density and follicular inflammation patterns in alopecia areata can be isolated by comparing the pathological surrogate with a reconstructed healthy scalp baseline.

Skin Monitoring: The pipeline could be adapted to clinical images to monitor lesions growth, border irregularity, and morphological changes in melanoma, ensuring that sensitive biometric data are never exposed

during the multi-institutional training required for rare cancer detection.

By preserving fine-grained markers—such as scaling in psoriasis, texture in eczema, or pigment distribution—while stochastically transforming global biometric geometry, the pipeline provides a robust solution for high-fidelity FL. This modularity is particularly vital for rare diseases where privacy constraints often lead to severe data scarcity, as it allows for the creation of standardized, de-identified synthetic datasets that retain full diagnostic utility.

5. Conclusion

This study presents a federated-ready framework that preserves privacy for dermatological analysis models. The critical tension between data privacy and diagnostic utility was addressed by integrating inversion-free FlowEdit with a counterfactual Segment-by-Synthesis pathology annotation procedure.

Our pilot results demonstrate that it is possible to decouple pathological signals from patient identity with high fidelity ($\text{IoU} > 0.67$) and effectively create a “Privacy Firewall” at the network edge. This approach enables the generation of GDPR-compliant Digital Twins, allowing institutions to participate in Federated Learning without exposing sensitive biometric data to gradient leakage risks. Future work will simulate a multi-client environment to quantify the convergence benefits of training on these noise-free synthetic labels.

References

- [1] A. Esteva *et al.*, “Dermatologist-level classification of skin cancer with deep neural networks,” *Nature*, vol. 542, no. 7639, pp. 115–118, Feb. 2017, doi: 10.1038/nature21056.
- [2] A. Kallipolitis *et al.*, “Skin image analysis for detection and quantitative assessment of dermatitis, vitiligo and alopecia areata lesions: a systematic literature review,” *BMC Med. Inform. Decis. Mak.*, vol. 25, no. 1, p. 10, Jan. 2025, doi: 10.1186/s12911-024-02843-2.
- [3] T. Ren *et al.*, “Grounded SAM: Assembling Open-World Models for Diverse Visual Tasks,” Jan. 25, 2024, *arXiv*: arXiv:2401.14159. doi: 10.48550/arXiv.2401.14159.
- [4] J. Geiping, H. Bauermeister, H. Dröge, and M. Moeller, “Inverting gradients - how easy is it to break privacy in federated learning?,” in *Proceedings of the 34th International Conference on Neural Information Processing Systems*, in NIPS ’20. Red Hook, NY, USA: Curran Associates Inc., Dec. 2020, pp. 16937–16947. Accessed: Jan. 26, 2026. [Online]. Available: <https://dl.acm.org/doi/10.5555/3495724.3497145>
- [5] V. Kulikov, M. Kleiner, I. Huberman-Spiegelglas, and T. Michaeli, “FlowEdit: Inversion-Free Text-Based Editing Using Pre-Trained Flow Models,” Jul. 22, 2025, *arXiv*: arXiv:2412.08629. doi: 10.48550/arXiv.2412.08629.
- [6] K. Moutselos and I. Maglogiannis, “Zero-shot Segmentation of Skin Conditions: Erythema with Edit-Friendly Inversion,” presented at the MICAD 2025, Nov. 2025. doi: 10.48550/arXiv.2508.01334.
- [7] G. A. Kaassis, M. R. Makowski, D. Rückert, and R. F. Braren, “Secure, privacy-preserving and federated machine learning in medical imaging,” *Nat. Mach. Intell.*, vol. 2, no. 6, pp. 305–311, Jun. 2020, doi: 10.1038/s42256-020-0186-1.
- [8] H. Hukkelås, R. Mester, and F. Lindseth, “DeepPrivacy: A Generative Adversarial Network for Face Anonymization,” in *Advances in Visual Computing*, G. Bebis, R. Boyle, B. Parvin, D. Koracin, D. Ushizima, S. Chai, S. Sueda, X. Lin, A. Lu, D. Thalmann, C. Wang, and P. Xu, Eds., Cham: Springer International Publishing, 2019, pp. 565–578. doi: 10.1007/978-3-030-33720-9_44.
- [9] R. Rombach, A. Blattmann, D. Lorenz, P. Esser, and B. Ommer, “High-Resolution Image Synthesis with Latent Diffusion Models,” in *2022 IEEE/CVF Conference on Computer Vision and Pattern Recognition (CVPR)*, New Orleans, LA, USA: IEEE, Jun. 2022, pp. 10674–10685. doi: 10.1109/CVPR52688.2022.01042.
- [10] R. Mokady, A. Hertz, K. Aberman, Y. Pritch, and D. Cohen-Or, “Null-text Inversion for Editing Real Images using Guided Diffusion Models,” Nov. 17, 2022, *arXiv*: arXiv:2211.09794. doi: 10.48550/arXiv.2211.09794.
- [11] Y. Lipman, R. T. Chen, H. Ben-Hamu, M. Nickel, and M. Le, “Flow Matching for Generative Modeling,” *ArXiv Prepr. ArXiv221002747*, 2022.
- [12] X. Liu, C. Gong, and Q. Liu, “Flow Straight and Fast: Learning to Generate and Transfer Data with Rectified Flow,” Sep. 07, 2022, *arXiv*: arXiv:2209.03003. doi: 10.48550/arXiv.2209.03003.
- [13] A. Kirillov *et al.*, “Segment Anything,” in *2023 IEEE/CVF International Conference on Computer Vision (ICCV)*, Oct. 2023, pp. 3992–4003. doi: 10.1109/ICCV51070.2023.00371.
- [14] L. Ke *et al.*, “Segment Anything in High Quality,” Oct. 23, 2023, *arXiv*: arXiv:2306.01567. doi: 10.48550/arXiv.2306.01567.
- [15] K. Delibasis, K. Moutselos, E. Vorgiazidou, and I. Maglogiannis, “Automated hair removal in dermoscopy images using shallow and deep learning neural architectures,” *Comput. Methods Programs Biomed. Update*, vol. 4, p. 100109, Jan. 2023, doi: 10.1016/j.cmpbup.2023.100109.
- [16] “Eczema on Face: Symptoms, Causes, Types & Treatment,” Cleveland Clinic. Accessed: Jan. 20, 2026. [Online]. Available: <https://my.clevelandclinic.org/health/diseases/24604-eczema-on-face>
- [17] “Dermnet.” Accessed: Jan. 20, 2026. [Online]. Available: <https://www.kaggle.com/datasets/shubhamgoel27/dermnet>